MECHANISM OF MODIFIED PEONY DECOCTION IN ALLEVIATING CONCURRENT LUNG AND INTESTINAL BARRIER INJURY IN ULCERATIVE COLITIS RATS VIA RHO/ROCK/NF-KB PATHWAY

X. Y. Zhan[1], H.Y. Xu[1], H. M. Zhang[1], Y. S. Jia[1], F. W. Wu[1], L. Y. Kong[2] and X. Yan[1*]

[1]College of Traditional Chinese Medicine, North China University of Science and Technology, Tangshan, 063210, Hebei, China;
[2]Department of Oncology, Affiliated Hospital of North China University of Science and Technology, Tangshan, 063000, Hebei, China.
*Corresponding author's Email: yanxintech8@126.com

ABSTRACT

Ulcerative colitis (UC) is characterized by its tendency to relapse and difficulty in cure. The Rho/ROCK/NF-κB pathway serves as a critical regulatory axis in UC. However, the mechanism by which traditional Chinese herbal compounds modulate this pathway to ameliorate concurrent lung and intestinal barrier injury remains incompletely elucidated. The aim of this study was to investigate therapeutic mechanism of modified peony decoction in alleviating lung–gut barrier damage in UC rats via Rho/ROCK/NF-κB pathway, thereby addressing the current gap in both therapeutic strategies and mechanistic research in this field. Thirty specific-pathogen-free adult male Wistar rats were subcutaneously injected with 8 mg of antigen emulsion in the groin area, followed by slow intra-colonic administration of a 2,4,6-trinitrobenzenesulfonic acid (TNBS)/50% ethanol mixture at 5 cm from the anus to establish the UC model. Successfully modeled rats were randomly divided into five groups (n=6 per group): the UC group (administered 10 mL/kg saline by gavage), the mesalazine group (MESA group, administered 0.5 g/kg mesalazine by gavage), the low-dose group (LD group, administered 6 g/kg modified peony decoction by gavage), the medium-dose group (MD group, administered 12 g/kg modified peony decoction by gavage), and the high-dose group (HD group, administered 24 g/kg modified peony decoction by gavage). All groups received daily gavage for 28 consecutive days. Additionally, six non-modeled rats served as the blank control group (BC group) and were administered 10 mL/kg saline by gavage. The distinctions in body weight (BW) and disease activity index (DAI) were analyzed after gavage treatment. Rat lung and colon tissues were collected for histopathological changes observed by HE staining, and F-actin (F-act), VE-cadherin (VE-cad), and ZO-1 was observed by immunofluorescence staining. Rho/ROCK/NF-κB pathway and key proteins of the mucosal barrier were detected by Western blotting. As against BC group, UC group demonstrated weight loss and increased DAI scores; lung and colon tissues exhibited disordered structure and inflammatory cell infiltration; the decreased expression intensity of F-act, VE-cad, and ZO-1, and increased p-Rho A, ROCK1, NF-κB, COX-2, and VEGF. As against UC group, MESA, LD, MD and HD groups exhibited increased BW and decreased DAI scores; the significant improved pathological damage of lung and colon tissues; the increased expression intensity of F-act, VE-cad, and ZO-1, and the decreased p-Rho A, ROCK1, NF-κB, COX-2, and VEGF. The HD group exhibited significant better improvement in all indicators than LD group and MD group (all $P<0.05$). UC rats exhibited significant concurrent injury to both the lung and intestinal barriers. Treatment with different doses of modified peony decoction resulted in increased body weight, reduced DAI scores, markedly improved histopathological damage in lung and colon tissues, enhanced expression intensities of F-actin, VE-cadherin, and ZO-1, along with decreased expression levels of p-RhoA, ROCK1, NF-κB, COX-2, and VEGF. The high-dose group demonstrated significantly greater improvement in all these indicators compared to the low- and medium-dose groups, showing that modified peony decoction alleviates lung-intestinal barrier injury in UC rats via the Rho/ROCK/NF-κB pathway.

Keywords: modified peony decoction; ulcerative colitis; concurrent lung and intestinal barrier injury; tight junction

https://doi.org/10.36899/JAPS.2026.4.0079 Published first online May 01, 2026

INTRODUCTION

Ulcerative colitis (UC) is inflammatory bowel disease (IBD) that differs from Crohn's disease. UC primarily affects the rectum and extends continuously to the proximal colon (Le Berre *et al.,* 2023). In contrast, Crohn's disease affects gastrointestinal tract, presenting with discontinuous transmural inflammatory lesions (Dolinger *et al.,* 2024). The

course of UC is chronic and relapsing, primarily characterized by symptoms such as diarrhea, mucopurulent and bloody stools, and abdominal pain, which significantly impair patients' quality of life (Kucharzik *et al.,* 2020). Pathogenesis of UC is highly complex, involving genetics, environment, immunity, and microbiota (Petagna *et al.,* 2020). It was revealed that UC is not confined to the intestine as an isolated condition but is closely associated with systemic immune dysregulation, often accompanied by extraintestinal organ damage (Lin *et al.,* 2022). Both the lung and the intestine are mucosal immune organs, interconnected via the circulatory system, lymphatic system, and gut microbial metabolites. Pulmonary barrier function is susceptible to remote regulation by intestinal inflammation, leading to interactive damage along the "gut–lung axis," which further exacerbates disease complexity and impacts prognosis, posing significant challenges for clinical management (Luo *et al.,* 2023a; Zhang *et al.,* 2024). Clinical treatments for UC often involve glucocorticoids, immunosuppressants, and biologics, yet therapeutic outcomes remain suboptimal (Sands *et al.,* 2023).

In TCM, UC falls under the categories of "abdominal pain", "hematochezia". The main cause is considered to be the stagnation of damp-heat in the large intestine, leading to qi stagnation, blood stasis. Modified peony decoction mainly consists of *Paeoniae Radix Alba*, *Scutellariae Radix*, *Coptidis Rhizoma*, *Rhei Radix et Rhizoma*, *Aucklandiae Radix*, *Arecae Semen*, *etc.*, with modifications based on clinical presentation (Jun *et al.,* 2019). In this formulation, *Paeoniae Radix Alba* serves as the sovereign herb (Jun), characterized by its sweet, bitter, and sour flavor and cold nature. It functions to nourish blood, harmonize blood circulation, soften the liver, alleviate urgency, and relieve pain, effectively addressing core symptoms of UC such as abdominal pain and tenesmus, while also providing a material basis for intestinal mucosal repair. *Scutellariae Radix*, *Coptidis Rhizoma*, and *Rhei Radix et Rhizoma*, with their bitter and cold properties, clear heat, dry dampness, purge fire, and detoxify. *Aucklandiae Radix* and *Arecae Semen* regulate qi, promote its movement, relieve stagnation, and alleviate middle-jiao pain. *Angelicae Sinensis Radix* nourishes and invigorates blood, assisting *Paeoniae Radix Alba* in harmonizing blood circulation and resolving stasis. A small amount of *Cinnamomi Cortex*, with its pungent and hot nature, prevents damage to the middle jiao by bitter-cold herbs and facilitates yang movement and qi transformation, collectively acting as assistant herbs. *Glycyrrhizae Radix et Rhizoma Praeparata cum Melle* harmonizes the various ingredients, tonifies the spleen, and boosts qi, serving as the envoy herb. Zeng and Li found that modified peony decoction could significantly alter the ultrastructure of primary cells from patients with adenomyosis to inhibit cell proliferation and induce apoptosis (Zeng and Li, 2017). Zhou *et al.* found that modified peony decoction used in the clinical remedy of restless legs syndrome could significantly improve clinical symptom scores and enhance patients' quality of life, sleep quality, and overall remedy effectiveness (Zhou *et al.,* 2024). Lee *et al.* found modified peony decoction is applied for premenopausal, perimenopausal, and postmenopausal menopausal-related diseases (Lee *et al.,* 2020). NF-κB activation can trigger immune responses in intestinal mucosal tissues. Wei *et al.* found peony decoction adopted for UC could significantly reduce inflammatory indices and inflammasome-related proteins, and it could also exert anti-necrotic effects via NF-κB p65 pathway (Wei *et al.,* 2021). Wu *et al.* noted that potential targets of peony decoction used in the remedy of UC mice included STAT3, IL-1β, IL-6, which could significantly alleviate intestinal mucosal damage and metabolic disorders in mice (Wu *et al.,* 2022a). Wang *et al.* confirmed that peony decoction alleviates colitis symptoms in UC mice by improving intestinal mucosal permeability and correcting the metabolic changes of M1 macrophages (Wang *et al.,* 2025). These studies have all confirmed the potential therapeutic effects of peony decoction on UC. However, intestinal inflammation is not limited to the intestine itself but may also spread to the lungs through the release of inflammatory mediators and blood circulation, causing pulmonary inflammatory responses. Mechanism of modified peony decoction in treating UC and improving concurrent lung and intestinal barrier injury remains to be verified.

It was hypothesized that the modified peony decoction alleviates pulmonary inflammation and repairs lung-intestinal barrier damage by modulating the Rho/ROCK/NF-κB signaling pathway, thereby inhibiting the release of intestinal inflammatory mediators and reducing the transmission of inflammatory signals to the lungs via systemic circulation. This work established the UC rat model using the immune complex method and analyzed influences of modified peony decoction on pathological changes, tight junction structure, and mucosal barrier function of rat lung-colon tissues. It aims to provide reference materials for understanding the potential mechanisms of concurrent lung and intestinal barrier injury after UC and the therapeutic effects of modified peony decoction.

MATERIALS AND METHODS

Construction of UC model: Thirty-six clean-grade adult male Wistar rats (100-120 g, Beijing Sipeifu Experimental Animal Co., Ltd., China) were used. The UC model was established following the method described by Xie *et al.* (Xie *et al.,* 2022). After the colonic mucosal epithelial cells from rabbits (Shanghai Enzyme Linked Co., Ltd., China) were cultured, the supernatant was collected and mixed with Freund's adjuvant (Sigma-Aldrich, USA) to prepare the antigen emulsion. Thirty rats were randomly selected and fed adaptively for 7 days, and were subcutaneously injected with 8 mg of the antigen emulsion in the inguinal region on days 7, 14, and 21. On day 28, after fasting for 48 hours, the rats were

anesthetized with 3% pentobarbital sodium (Sigma-Aldrich, USA) at 30 mg/kg via intraperitoneal injection. A gavage needle coated with paraffin oil was used to slowly instill a mixture of 100 mg/kg trinitrobenzene sulfonic acid (Sigma-Aldrich, USA) + 50% ethanol (Nanjing Chemical Reagent Co., Ltd., China) into a 5 cm section of the colon taken from the rat's anus. The anus was clamped and the rat was hung upside down for 3 minutes. The rat was then placed in a supine position in a breeding cage, allowed to eat and drink freely after full recovery, and regularly observed for mental state, body weight (BW), stool condition, and survival. All animal procedures were approved by the Institutional Animal Care and Use Committee of North China University of Science and Technology, conducted in accordance with guidelines.

Grouping and remedy: Six rats that were not subjected to modeling were used as BC group and received a gavage treatment of 10 mL/kg saline. The 30 successfully modeled rats were randomly grouped, with 6 rats in each:
UC group received a gavage treatment of 10 mL/kg saline after modeling;
MESA group received a gavage treatment of 0.5 g/kg mesalamine (Koohi *et al.,* 2023) after modeling;
LD group received a gavage treatment of 6 g/kg modified peony decoction after modeling;
MD group received a gavage treatment of 12 g/kg modified peony decoction after modeling;
HD group received a gavage treatment of 24 g/kg modified peony decoction after modeling.
All groups were given gavage continuously for 28 days.

General observation: The general condition, stool condition, and hematochezia of the rats were observed. BW changes were recorded on days 0, 1, 7, 14, 21, and 28, and DAI assessed disease activity status of rats. The DAI scoring criteria (Zhuang *et al.,* 2021) were as follows: a weight loss score of 0%, normal stool condition, and negative occult blood in stool (-) was scored as 0; 1-5%, loose, and (+): 1; 6-10%, semi-liquid, and (++): 2; 11-15%, liquid, and significant blood in stool: 3; >15%, liquid, and significant blood in stool: 4. DAI score=(weight loss score + stool condition score + hematochezia score) / 3.

Pathological observation: The day after the last gavage, the rats were anesthetized as described above. Abdomen was opened along the midline, and a 1 cm section of the typical lesion colon tissue from 5-15 cm above the anus was taken; the upper right lobe of the lung was collected after cutting the sternum. The colon contents and lung tissue blood were washed with pre-cooled saline, and tissues were fixed in 10% neutral formalin solution, dehydrated with gradient alcohol, embedded in paraffin, and sectioned into 4 μm thick paraffin slices. According to the instructions of the H&E kit (Beijing Solarbio Co., Ltd., China), the paraffin slices were baked at 65℃ for 2 hours, dewaxed and rehydrated with xylene and gradient alcohol, stained in hematoxylin solution for 5 minutes, rinsed twice; differentiated for 2 seconds, rinsed twice; stained in eosin solution for 2 minutes, rinsed twice; dehydrated with gradient alcohol and xylene. After sealing with neutral gum, the pathological morphological changes were subjected to observation adopting the SZX10 optical microscope (Olympus, Japan). Colonic tissues were primarily evaluated for mucosal integrity, degree of inflammatory cell infiltration, glandular destruction, and crypt abscess formation, with the extent of tissue damage assessed using the modified mucosal damage index (MDI) score. Pulmonary tissues were examined for alveolar structural integrity, thickness of alveolar septa, inflammatory cell infiltration, and damage to the bronchial mucosal epithelium.

1 mm^3 of lung tissue was fixed in 2.5% glutaraldehyde and 1% osmium acid (both from Nanjing Chemical Reagent Co., Ltd., China), and ultra-thin sections were prepared. TEM examined the ultrastructure of pulmonary epithelial cells, with a focus on evaluating the continuity and integrity of tight junctions, mitochondrial morphology, ciliary structure, and damage to cytoplasmic organelles, in order to characterize the type and extent of ultrastructural injury in these cells.

Immunofluorescence staining observation: Paraffin sections were taken and processed for dewaxing and rehydration, followed by antigen retrieval. The sections were incubated with 3% hydrogen peroxide in the dark at 25℃ for 20 minutes and then rinsed with PBS. Normal goat serum blocking solution (Sigma-Aldrich, USA) was adopted to block the sections at 25℃ for 30 minutes. Primary antibodies against F-act, VE-cad, and ZO-1 (Abcam, UK) were adopted, incubation overnight at 4℃. Biotinylated goat anti-rat IgG antibody (Abcam, UK) was adopted, incubation at 37℃ for 30 minutes in a humidified chamber. SABC-Cy3 (Beijing Baiao Laibo Technology Co., Ltd., China) was adopted, incubation in the dark at 25℃ for 30 minutes, rinsed and mounted with glycerin. DAPI (Thermo Fisher, USA) was adopted, incubation in the dark for 5 minutes for nuclear counterstaining. After adding an anti-fade agent, they were mounted and subjected to observation adopting a CX33 fluorescence microscope (Olympus, Japan) for immunofluorescence staining.

Western blotting analysis: Lung and intestinal tissues were collected and total protein was subjected to extraction adopting RIPA buffer (Thermo Fisher, USA). The concentration was subjected to determination adopting the

bicinchoninic acid assay (Thermo Fisher, USA). An equal amount (50 μg) of total protein was loaded and separated by SDS-PAGE. Proteins were transferred onto a PVDF membrane and blocked at 25°C for 2 hours. The membrane was incubated overnight at 4°C with primary antibodies (1:1000; Abcam, UK) against Rho A, p-Rho A, ROCK1, NF-κB, COX-2, and VEGF. After washing, the membrane was incubated with HRP-conjugated IgG secondary antibody (1:5000; Abcam, UK) at 25°C for 2 hours. The membranes were washed and the protein signals were detected adopting a WD-9423B fully automatic chemiluminescence imager (Beijing Liu Yi Biotechnology Co., Ltd., China). β-actin served as a reference to compute relative expression (RE). Western blot analysis was independently repeated three times to ensure reproducibility of the results.

Statistical processing: Employing *SPSS 23.0*, datasets underwent normality testing and homogeneity of variance testing. Normally distributed continuous data with homogeneous variance, including colonic tissue damage scores, inflammatory cytokine levels, and protein expression levels, were expressed as $\bar{x}\pm s$ and were compared using one-way ANOVA. Following ANOVA, Tukey's honestly significant difference test was applied for pairwise comparisons to correct for multiple testing errors. Distinctions were statistically meaningful when $P<0.05$.

RESULTS

Contrast of general condition of rats: The BW changes at different time points after modeling were compared (Figure 1A). It was found that the BW of BC group gradually raised, while the BW of UC, MESA, LD, MD, and HD groups decreased on the first day after modeling and then displayed a gradual increasing trend. Body weights were observed different among all groups at all time points except Day 0 ($P<0.05$). Versus UC group, BC group exhibited higher body weight starting from postoperative Day 1 ($P<0.05$). The DAI scores at different time points after modeling were then compared (Figure 1B). It was found that the DAI scores of UC, MESA, LD, MD, and HD groups significant raised on the first day after modeling and then displayed a gradual decreasing trend. The DAI scores of HD group were close to those of MESA group. Drastic differences in DAI scores existed among all groups at postoperative days 1, 7, and 14 ($P<0.05$). The BC group exhibited significantly lower DAI scores from day 1 to day 14 versus UC ($P<0.05$).

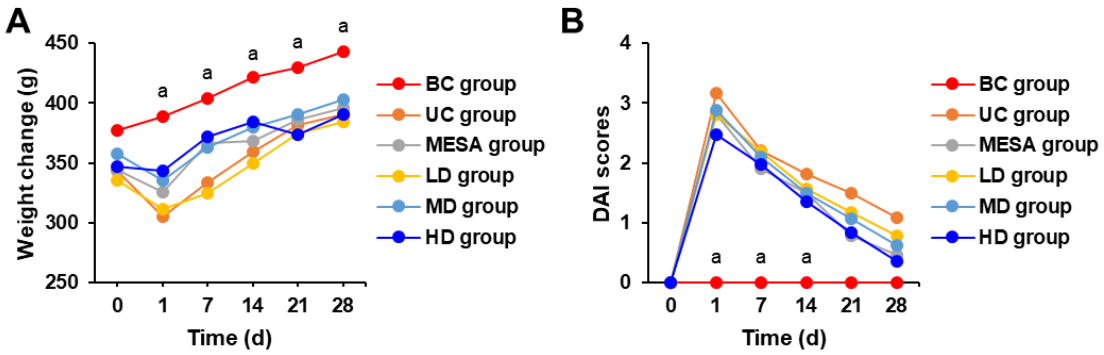

Figure 1. Changes in the general condition of rats. A:BW-time change curve; B: DAI score-time change curve. [a]*P*<0.05 vs. UC group;

Contrast of pathological morphology: Lung tissue pathological morphology changes were observed by HE staining and electron microscopy (Figure 2 and Figure 3). It was found that the lung tissue contour in BC group was clear, no edema or fibrosis. In UC group, the lung tissue was significantly congested, with many inflammatory cell infiltrations in the lung interstitium, increased alveolar septa, unclear structure, and a small amount of fibrous tissue proliferation. The degree of lung tissue changes in MESA, LD, MD, and HD groups was improved in contrast to UC group, with MESA group and HD group showing the most significant improvement. A small amount of fibrous tissue proliferation in the lung interstitium, some alveolar tissue structure had recovered.

In Figure 4, the colon mucosa in BC group was intact with neatly arranged glands, and no inflammatory cell infiltration. In UC group, the colon mucosa exhibited varying degrees of defect or necrosis, with inflammatory cell infiltration forming ulcers. The degree of colon tissue lesion in MESA, LD, MD, and HD groups was improved in contrast to UC group, with MESA group and HD group showing the most significant improvement in colon mucosa damage, with slight cell infiltration. The mean colonic pathological injury scores were 0.17 ± 0.28 in the BC group, 2.89 ± 0.505 in the UC group, 1.33 ± 0.47 in the MESA group, 1.83 ± 0.75 in the LD group, 1.72 ± 0.49 in the MD group, and 1.39 ± 0.39 in the HD group. One-way ANOVA revealed a highly statistically significant difference in mean scores

among the groups (F=27.79, P<0.001). Post-hoc analysis using Tukey's HSD test showed that compared to the BC group, the other five groups had significantly higher colonic pathological injury scores (P<0.05). Compared to the UC group, the MESA, LD, MD, and HD groups exhibited significantly lower pathological injury scores (P<0.05). The MESA and HD groups showed the lowest scores, with no statistically significant difference between them (P>0.05).

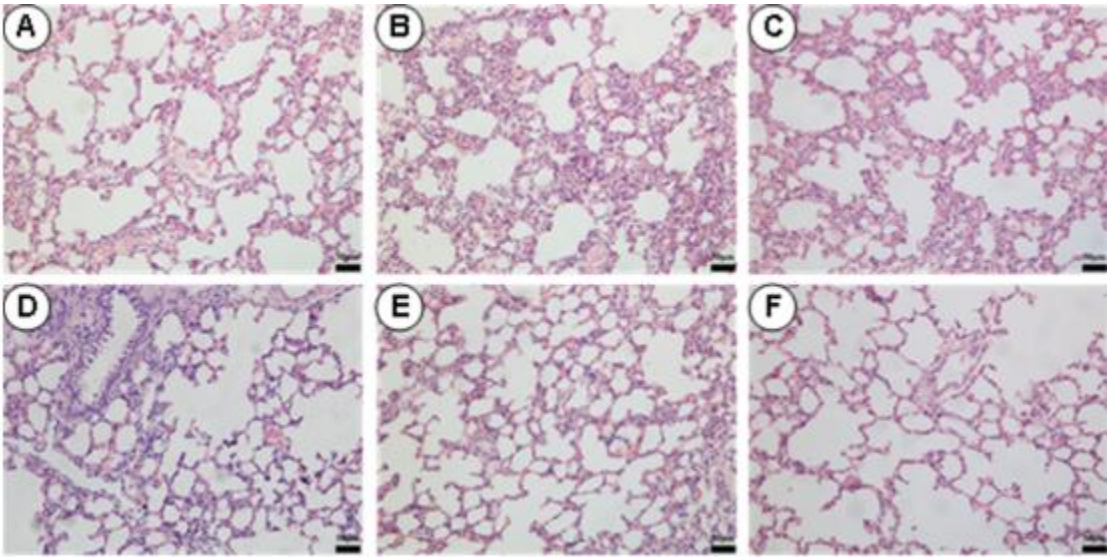

Figure 2. HE staining of lung tissue in rats (200×). A: BC; B: UC; C: MESA; D: LD; E: MD; F: HD.

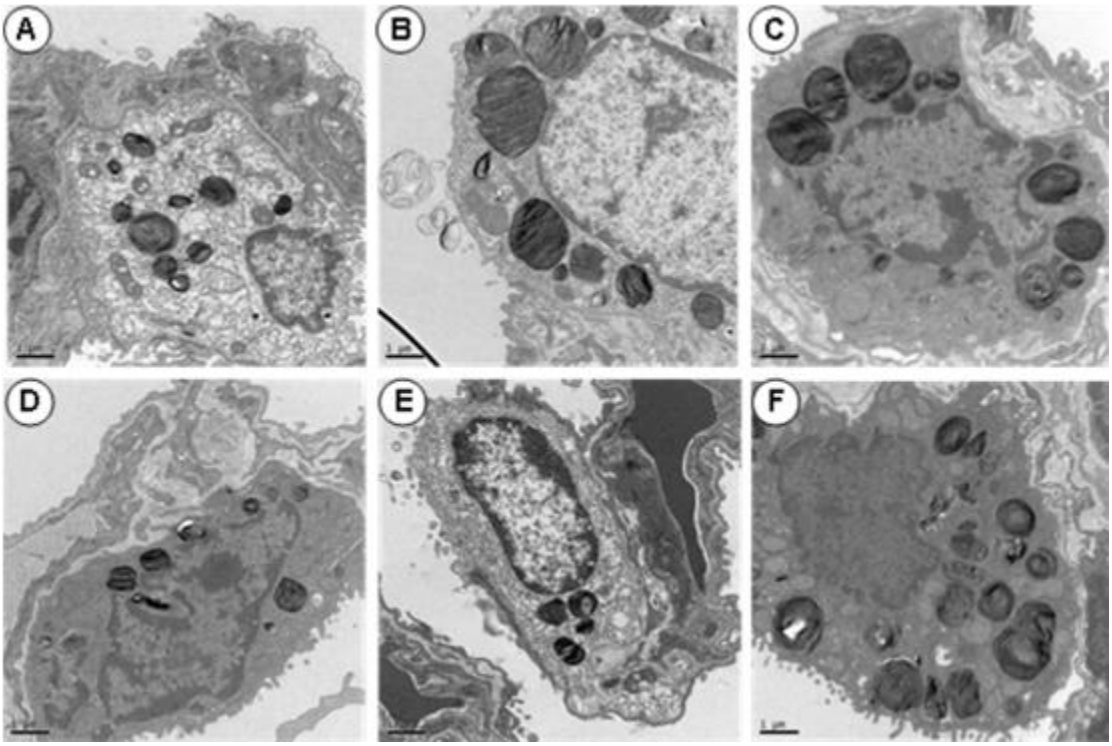

Figure 3. Electron microscopy observation of lung tissue in rats (200×). A: BC; B: UC; C: MESA; D: LD; E: MD; F: HD.

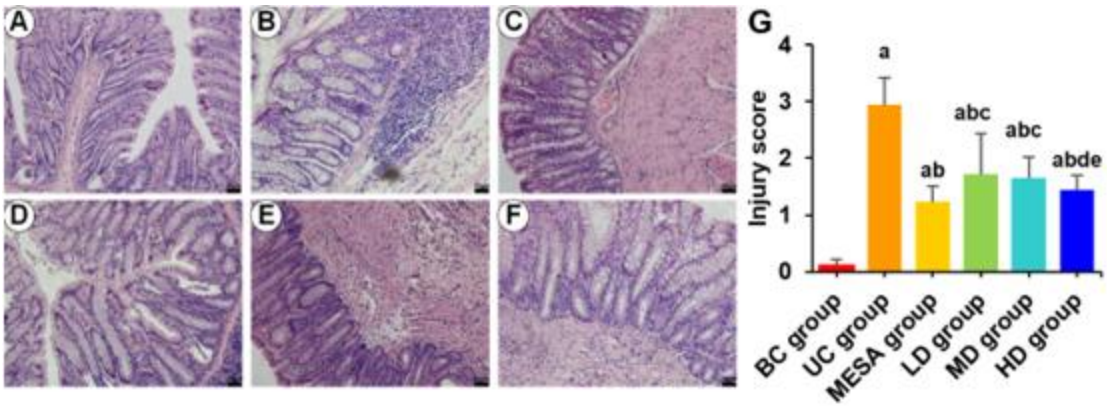

Figure 4. HE staining observation of colon tissue in rats (200×). A: BC; B: UC; C: MESA; D: LD; E: MD; F: HD.
Note: [a]*P*<0.05 vs. BC; [b]*P*<0.05 vs. UC; [c]*P*<0.05 vs. MESA; [d]*P*<0.05 vs. LD; [e]*P*<0.05 vs. MD (in all Figures).

Contrast of F-act, VE-cad, and ZO-1: In Figure 5, there was varying degrees of F-act, VE-cad, and ZO-1 in rats. The expression intensity was significantly reduced and was significantly lower in UC group; that in MESA, LD, MD, and HD groups was significantly higher relative to UC group ($P<0.05$). With increasing dosage, the expression intensity in LD, MD, and HD groups gradually raised.

In Figure 6, there were varying degrees of F-act, VE-cad, and ZO-1 in the colon tissue of rats. Expression intensity was significantly reduced and was significantly lower in UC group; that in MESA, LD, MD, and HD groups was markedly higher relative to UC group ($P<0.05$). With increasing dosage, the expression intensity in LD, MD, and HD groups also exhibited a gradually increasing trend.

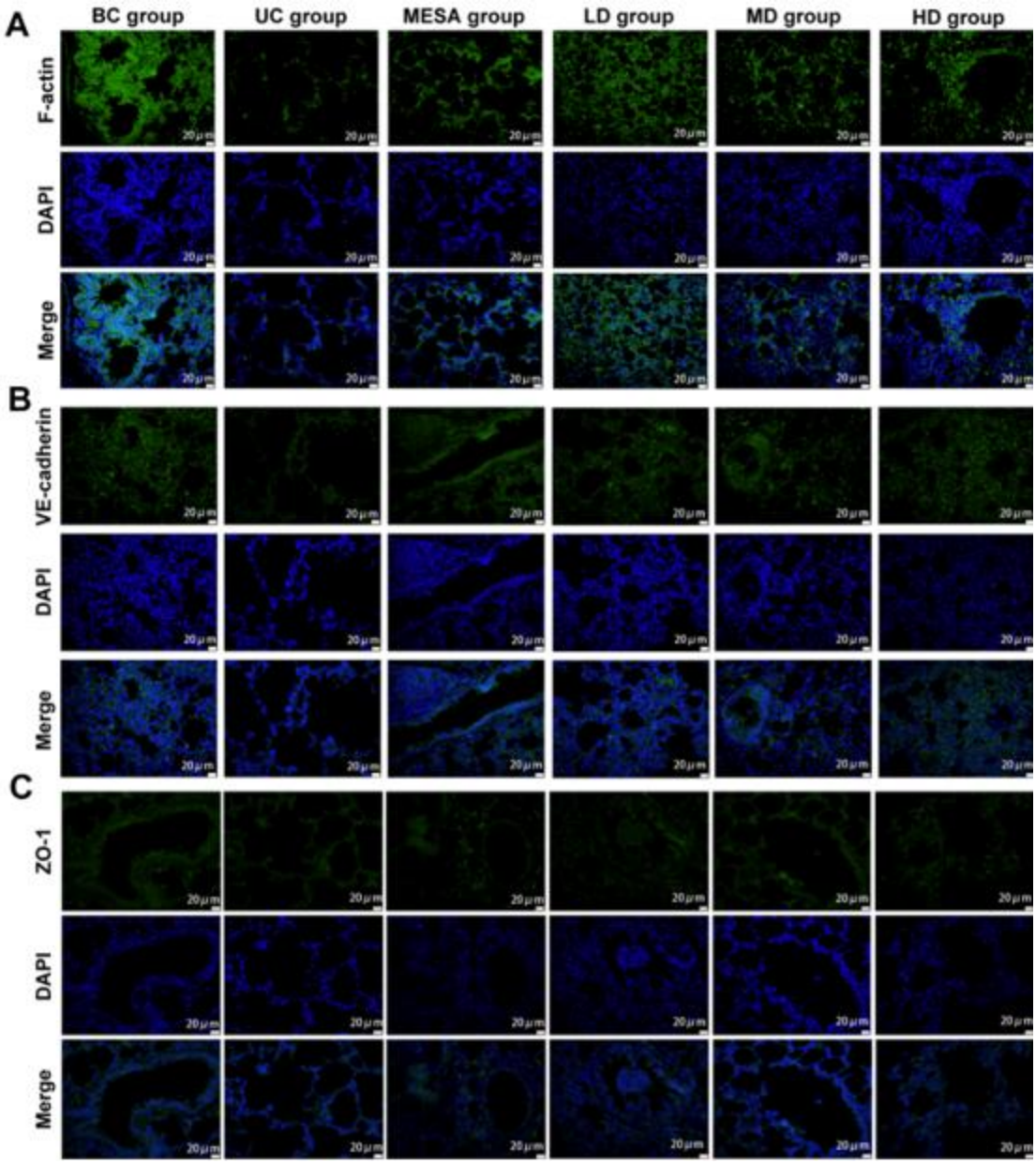

Figure 5. Expression of F-act, VE-cad, and ZO-1 in rat lung tissue (400×). A: immunofluorescence staining for F-act; B: immunofluorescence staining for VE-cad; C: immunofluorescence staining for ZO-1; D: relative F-act; E: relative VE-cad; F: relative ZO-1.

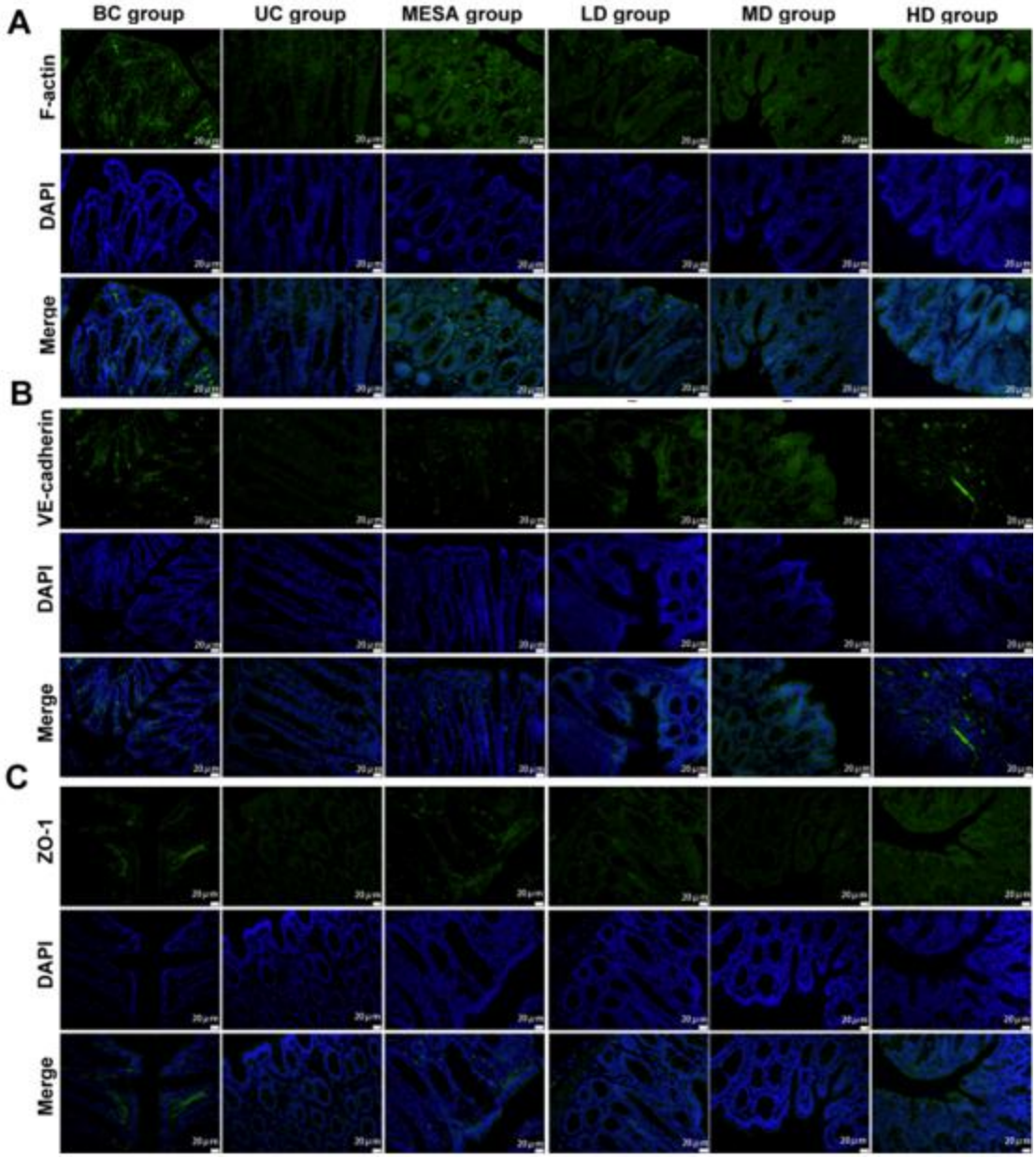
A
BC group
UC group
MESA group
LD group
MD group
HD group
F-actin
DAPI
Merge
B
VE-cadherin
DAPI
Merge
C
ZO-1
DAPI
Merge

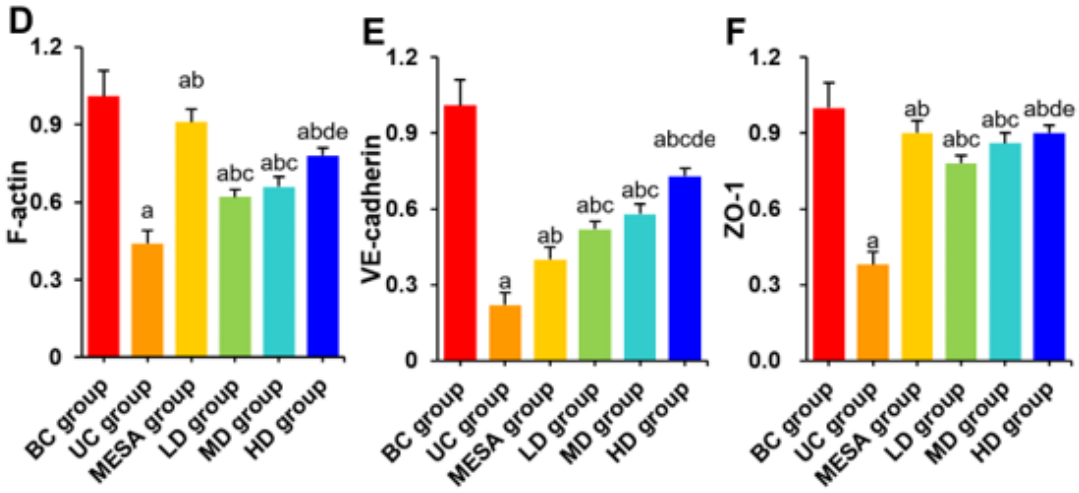

Figure 6. Expression of F-act, VE-cad, and ZO-1 in rat colon tissue (400×). A: immunofluorescence staining for F-act; B: immunofluorescence staining for VE-cad; C: immunofluorescence staining for ZO-1; D: relative F-act; E: relative VE-cad; F: relative ZO-1.

Contrast of key protein expression in Rho/ROCK/NF-κB pathway: In Figure 7, p-Rho A, ROCK1, and NF-κB were markedly raised and were markedly higher in UC group; those in MESA, LD, MD, and HD groups were markedly lower versus UC ($P<0.05$). With increasing dosage, p-Rho A and ROCK1 in LD group, MD group, and HD group demonstrated a gradually decreasing trend. NF-κB in the lung tissue of MD group was higher relative to LD group and HD group. No significant distinction was noted in the protein expression in colon tissue of LD, MD, and HD groups ($P>0.05$).

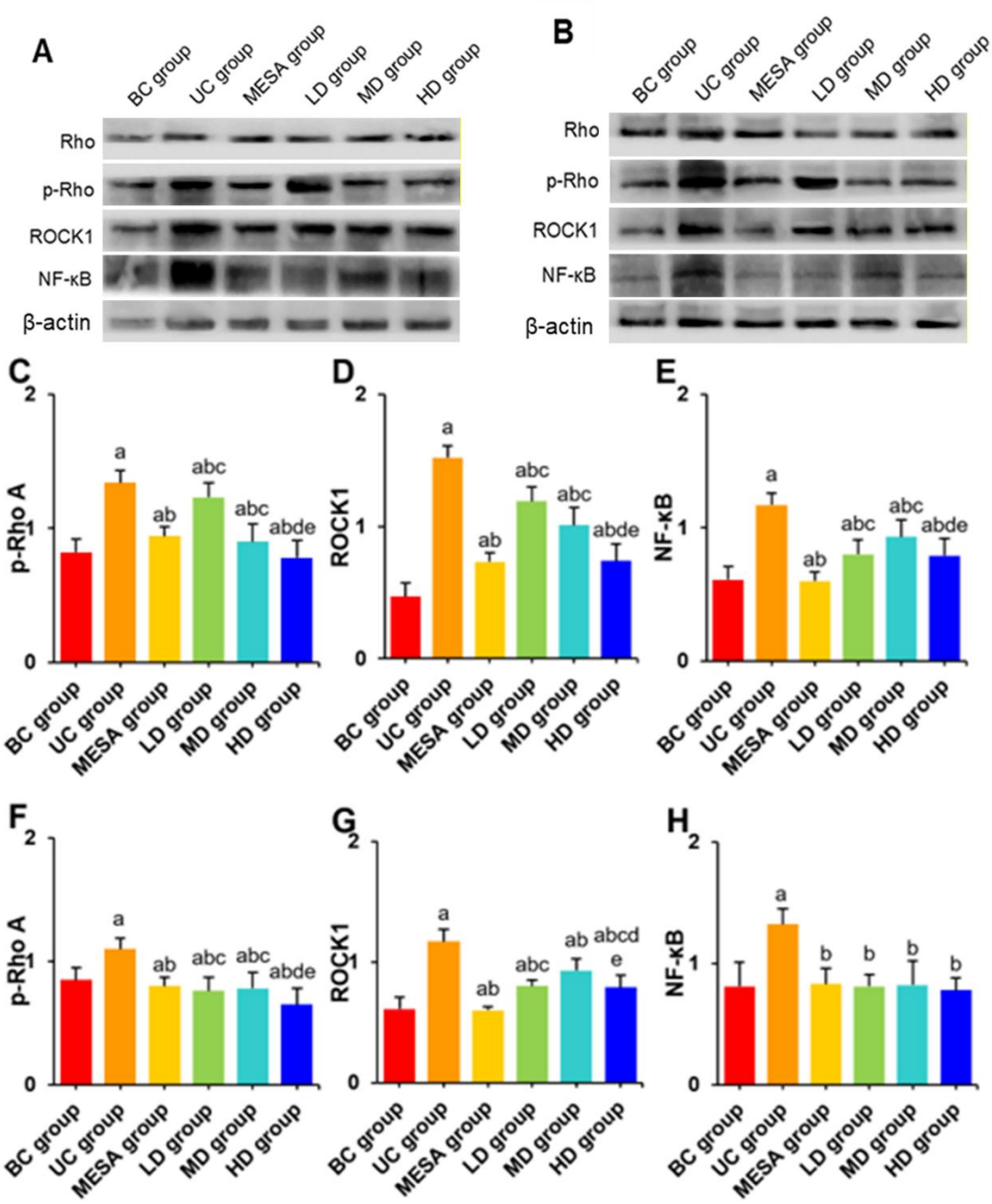

Figure 7. Expression of key proteins in the Rho/ROCK/NF-κB pathway in rat lung and intestinal tissues. A: Western blotting for lung tissue proteins; B: Western blotting for colon tissue proteins; C: relative p-Rho A in lung; D: relative ROCK1 in lung; E: relative NF-κB in lung; F: relative p-Rho in colon; G: relative ROCK1 in colon; H: relative NF-κB in colon.

Contrast of key protein expression in the mucosal barrier: In Figure 8, the levels of COX-2 and VEGF were markedly raised and were markedly higher in UC group; those in MESA, LD, MD, and HD groups were markedly lower versus UC ($P<0.05$). No significant distinction was noted in COX-2 in the lung and intestinal tissues, and in VEGF in lung tissue of the MESA group, LD group, and MD group ($P>0.05$); COX-2 and VEGF in lung and intestinal tissues of HD group were markedly lower relative to MD and HD groups ($P<0.05$).

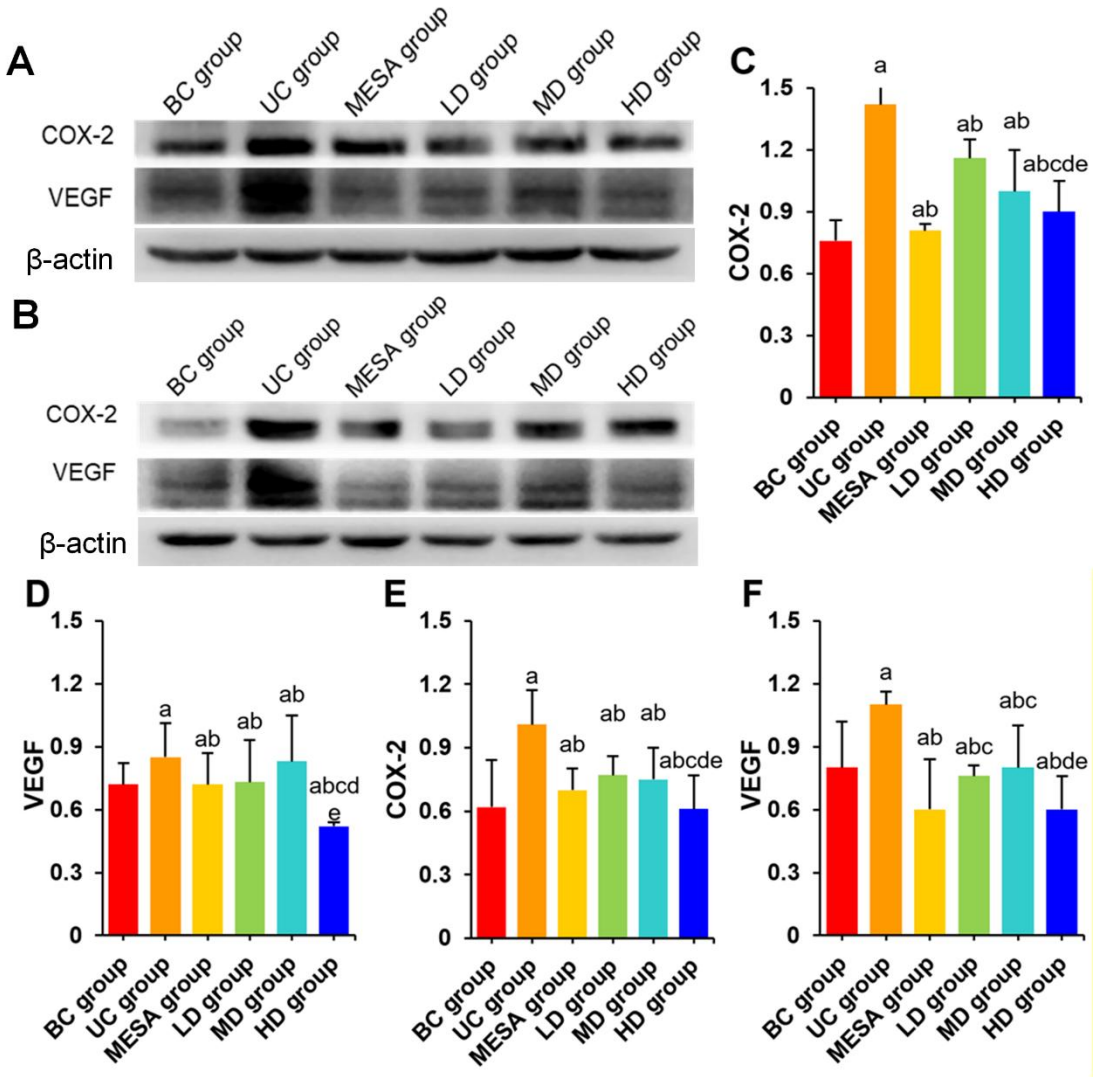

Figure 8. Expression of key proteins in the mucosal barrier of rat lung and intestinal tissues. A: Western blotting for lung tissue proteins; B: Western blotting for colon tissue proteins; C: relative COX-2 in lung; D: relative VEGF in lung; E: relative COX-2 in colon; F: relative VEGF in colon.

DISCUSSION

Our results revealed that UC rats had decreased BW and raised DAI scores relative to normal rats. Additionally, through HE staining experiment, colonic mucosa of UC rats revealed different degrees of defect or necrosis, accompanied by inflammatory cell infiltration and ulcer formation. The main lesions of UC are in the colonic mucosa and submucosa, characterized by inflammatory cell infiltration and ulcers (Wangchuk *et al.,* 2024). Hence, a reliable UC rat model was successfully established, laying foundation for subsequent experiments. Then, post to modified peony decoction treatment, the BW of UC rats raised, and the DAI scores decreased, with considerable enhancement in colonic mucosal necrosis, inflammatory cell infiltration, and ulcer changes. TCM believes that UC may be related to damp-heat and disharmony of qi and blood (Zheng *et al.,* 2022; Wu *et al.,* 2022b). Modified peony decoction is a commonly used prescription. Modified peony decoction can improve intestinal inflammatory symptoms through mechanisms such as clearing heat, regulating qi and blood (Wu *et al.,* 2023). The above mechanisms are related to suppressing intestinal inflammation, regulating immune function, and improving intestinal microcirculation.

UC shows persistent or recurrent diarrhea and bloody stools as the main clinical manifestations. As reported, patients with inflammatory bowel disease tend to develop pulmonary symptoms, with about 50% of patients showing respiratory symptoms such as dyspnea, cough, or sputum production (Marvisi *et al.,* 2019). From modern embryological

studies, structural origin of the lung and intestine is the same, and both the respiratory and gastrointestinal mucosa are part of the common mucosal immune system (Paul *et al.,* 2022). Our results revealed that lung tissue structure of UC rats changed markedly, with inflammatory cell infiltration and pulmonary interstitial fibrosis, and the colon tissue also exhibited inflammatory cell infiltration with raised pathological damage scores. The noted results indicated that UC rats have concurrent damage to the pulmonary and intestinal mucosal barriers. Modern pharmacological studies have confirmed that traditional Chinese medicine can protect intestinal mucosal barrier through mechanisms such as regulating intestinal motility, promoting damaged mucosa repair, improving microcirculation, maintaining intestinal flora balance, and antioxidant stress (Liu *et al.,* 2022; Wang *et al.,* 2024). This study found that modified peony decoction can markedly improve the structural damage of lung and colon tissues in UC rats and reduce inflammatory cell infiltration. The connection structure of colonic epithelial cells and endothelial cells is key to the composition of the intestinal mechanical barrier, with main components including Claudin 5, ZO, and VE-cad (Jiang *et al.,* 2021). Outside the cell, transmembrane proteins interact with transmembrane proteins on adjacent cells to close cell pores; inside the cell, ZO protein families connect and fix; subsequently, they form the fascia structure between adjacent intestinal epithelial cells (Assimakopoulos *et al.,* 2020). This effectively prevents bacteria and antigens from entering intestinal mucosal lamina propria and avoids abnormal immune reactions of the intestinal mucosa. ZO-1 plays an intermediary role in tight junctions, and its combination with the carboxyl terminus of the transmembrane protein Occludin can form the basic structure of tight junctions (Kuo *et al.,* 2022). F-act is the main component of intracellular microfilaments, providing structural support for the cytoskeleton, and it can maintain the tight connection between cells by interacting with cell connection proteins (Chanez-Paredes *et al.,* 2024). VE-cad is an important adhesion connection protein, maintaining the tight connection between cells through calcium ion-dependent interactions (Bandyopadhyay *et al.,* 2021). Expression intensity of F-act, VE-cad, and ZO-1 in lung and colon tissues of UC rats was markedly reduced. It is speculated that the reduction in F-act, VE-cad, and ZO-1 is the pathological basis for the destruction of the intestinal mucosal tight junction structure and may also be key to UC intestinal epithelial barrier function damage and raised permeability. Scutellaria baicalensis and Coptis chinensis are both components of modified peony decoction. Cui *et al.* found Scutellaria baicalensis extract SP2-1 markedly reduces the BW loss and DAI scores, and repair the damaged colonic mucosal barrier by suppressing the release of pro-inflammatory cytokines and upregulating the expression of ZO-1, Occludin, and Claudin-5 (Cui *et al.,* 2021). Xie *et al.* found that Coptis chinensis gavage could increase the abundance of *Blautia*, etc. in the rat intestine, and protect the integrity of the intestinal tight junction structure by suppressing inflammatory reactions, thereby preventing intestinal barrier damage (Xie *et al.,* 2022). Zhou *et al.* found that Coptis chinensis alkaloids could reverse the intestinal wall swelling and inflammatory cell infiltration in colitis mice, and restore integrity of colonic mucosa by upregulating Claudin 1, etc (Zhou *et al.,* 2023). This indicates that modified peony decoction can regulate the expression of F-act, VE-cad, and ZO-1 in pulmonary and intestinal tissues through various pharmacological actions, thereby protecting the tight junction structure of the pulmonary and intestinal barriers, maintaining the normal function of the pulmonary and intestinal barriers, and repairing damaged tissues.

Mucosal injury-induced increase in intestinal permeability exacerbates bacterial translocation, disrupts intestinal homeostasis, and triggers inflammation (Di Vincenzo *et al.,* 2024). The Rho/ROCK pathway plays a role in regulating cytoskeletal dynamics and maintaining intestinal epithelial cell junctions, with phosphorylation of myosin light chain in this pathway being associated with increased intestinal endothelial permeability (Kimura *et al.,* 2021; Xu and Lin, 2024; Liu *et al.,* 2020). Zhang *et al.* induced a UC rat model using TNBS and observed significantly elevated expression of p-RhoA and ROCK1 in colonic tissues (Zhang *et al.,* 2021). Similarly, this study found that the expression levels of p-RhoA and ROCK1 in the lung and colonic tissues of UC rats were significantly higher than those in the control group (P<0.05). The Rho/ROCK pathway can activate NF-κB (Yan *et al.,* 2021), and inhibition of the NF-κB pathway promotes colonic mucosal repair (Zhou *et al.,* 2023). This study demonstrated that after administration of modified peony decoction, the levels of p-RhoA, ROCK1, and NF-κB in UC rats were significantly reduced. Activation of NF-κB promotes the release of IL-1, IL-6, and TNF-α, forming an inflammatory cascade (Shostak *et al.,* 2021). Previous studies noted that paconiflorin, peony decoction, and emodin exert anti-inflammatory effects, promote the restoration of intestinal mucosal homeostasis, and inhibit NF-κB in different models (Wang *et al.,* 2022; Chen *et al.,* 2024; Luo *et al.,* 2022). The modified peony decoction demonstrated reparative effects on lung and intestinal tissues, improving the morphological structure of damaged tissues and restoring barrier integrity. This reparative effect is likely mediated through the Rho/ROCK/NF-κB pathway, leading to the suppression of inflammatory responses. The regulation of this pathway by the modified peony decoction represents a key mechanism underlying its anti-inflammatory and protective actions. The regulatory function and reparative effects are interrelated and mutually reinforcing, with the reparative role being indispensable to its overall protective efficacy.

Granulation tissue is required for tissue repair following damage, and the deposition of connective tissue matrix, fibroblasts, and angiogenesis are key to restoring oxygen and nutrient supply to the damaged tissue (Liu *et al.,* 2025). VEGF is a potent angiogenic factor that can promote the proliferation and construction of blood vessels by endothelial

cells. In the intestinal barrier, VEGF and COX-2 may maintain intestinal barrier by promoting angiogenesis (Yin *et al.,* 2021). Kim *et al.* induced a colitis model and found that COX-2 in colon tissue was raised (Kim *et al.,* 2017). Şen *et al.* indicated that VEGF and COX-2 are markers of UC severity, with their expression upregulated in colonic tissue (Şen *et al.,* 2023). Our work indicated the same, revealing that COX-2 and VEGF act in regulation of concurrent pulmonary and intestinal barrier damage in UC. Subsequently, this study found that after gavage with modified peony decoction, COX-2 and VEGF in lung and colon tissues of UC rats were markedly reduced. There are currently no studies confirming the potential effects of peony decoction on COX-2 and VEGF in inflammatory bowel disease. However, Luo *et al.* found that peony and licorice decoction could inhibit the expression of COX-2 in a migraine animal model and exert analgesic effects (Luo *et al.,* 2023b). Zhang *et al.* found peony and licorice decoction could inhibit the expression of VEGF in serum and brain tissue to improve cerebral ischemia-reperfusion injury in rats (Zhang *et al.,* 2016). The above results show that modified peony decoction can improve the pulmonary and intestinal barrier function damage in UC rats by suppressing COX-2 and VEGF. In addition, Luo *et al.* indicated that Gram-positive bacteria promote UC through the MDP-NOD2 pathway, and paeoniflorin can inhibit the infiltration of Gram-positive bacteria in the intestine, thereby alleviating the disease process (Luo *et al.,* 2021). Hence, effects of modified peony decoction on the intestinal metabolism and microbiota structure in UC rats require to be revealed.

Conclusion: Modified peony decoction promotes repair of pulmonary and intestinal mucosal epithelial structures in UC rats and enhance concurrent damage of pulmonary and intestinal mucosa by suppressing Rho/ROCK/NF-κB pathway and COX-2 and VEGF expression.

Author's contribution: Conception and study design: Xinyu Zhan and Xin Yan; data acquisition and analysis: Xinyu Zhan, Huiyan Xu, Haimei Zhang, Yongsen Jia, Fanwu Wu, Lingyu Kong and Xin Yan; manuscript draft, editing and revision: Xinyu Zhan and Xin Yan. All authors wrote and approved the final manuscript.

Animal Ethics: All experiments were approved by Ethics Committee of North China University of Science and Technology (Tangshan, China), and in accordance with the Guide for the Care and Use of Laboratory Animals published by the United States National Institutes of Health.

Funding: This work was supported by National Natural Science Foundation Youth Fund Project (81704059) and Hebei Natural Science Foundation (H2022209057).

REFERENCES

Assimakopoulos, S.F., K. Akinosoglou, A.L. de Lastic, A. Skintzi, A. Mouzaki, and C.A. Gogos (2020). The Prognostic Value of Endotoxemia and Intestinal Barrier Biomarker ZO-1 in Bacteremic Sepsis. Am J Med Sci. 359(2): 100–107. https://doi.org/10.1016/j.amjms.2019.10.006

Bandyopadhyay, C., L. Schecterson, and B.M. Gumbiner (2021). E-cadherin activating antibodies limit barrier dysfunction and inflammation in mouse inflammatory bowel disease. Tissue Barriers. 9(4): 1940741. https://doi.org/10.1080/21688370.2021.1940741

Chanez-Paredes, S.D., S. Abtahi, J. Zha, E. Li, G. Marsischky, L. Zuo, M.J. Grey, W. He, and J.R. Turner (2024). Mechanisms underlying distinct subcellular localization and regulation of epithelial long myosin light-chain kinase splice variants. J Biol Chem. 300(2): 105643. https://doi.org/10.1016/j.jbc.2024.105643

Chen, S., P. Kang, Z. Zhao, H. Zhang, J. Li, K. Xu, D. Gong, F. Jiao, H. Wang, and M. Zhang (2024). Danggui-Shaoyao-San (DSS) ameliorates the progression of osteoarthritis via suppressing the NF-κB signaling pathway: an in vitro and in vivo study combined with bioinformatics analysis. Aging (Albany NY). 16(1): 648–664. https://doi.org/10.18632/aging.205410

Cui, L., X. Guan, W. Ding, Y. Luo, W. Wang, W. Bu, J. Song, X. Tan, E. Sun, Q. Ning, G. Liu, X. Jia, and L. Feng (2021). Scutellaria baicalensis Georgi polysaccharide ameliorates DSS-induced ulcerative colitis by improving intestinal barrier function and modulating gut microbiota. Int J Biol Macromol. 166: 1035–1045. https://doi.org/10.1016/j.ijbiomac.2020.10.259

Dolinger, M., J. Torres, and S. Vermeire (2024). Crohn's disease. Lancet. 403 (10432): 1177–1191. https://doi.org/10.1016/S0140-6736(23)02586-2

Di Vincenzo, F., A. Del Gaudio, V. Petito, L.R. Lopetuso, and F. Scaldaferri (2024). Gut microbiota, intestinal permeability, and systemic inflammation: a narrative review. Intern Emerg Med. 19(2): 275–293. https://doi.org/10.1007/s11739-023-03374-w

Jiang, Y., J. Song, Y. Xu, C. Liu, W. Qian, T. Bai, and X. Hou (2021). Piezo1 regulates intestinal epithelial function by affecting the tight junction protein claudin - 1 via the ROCK pathway. Life Sci. 275: 119254.

https://doi.org/10.1016/j.lfs.2021.119254

Jun, J.H., H.W. Lee, J. Choi, T.Y. Choi, J.A. Lee, H.Y. Go, and M.S. Lee (2019). Perceptions of using herbal medicines for managing menopausal symptoms: a web - based survey of Korean medicine doctors. Integr Med Res. 8(4): 229–233. https://doi.org/10.1016/j.imr.2019.08.004

Kim, D.S., S.H. Kim, J.Y. Kee, Y.H. Han, J. Park, J.G. Mun, M.J. Joo, Y.D. Jeon, S.J. Kim, S.H. Park, S.J. Park, J.Y. Um, and S.H. Hong (2017). Eclipta prostrata Improves DSS-Induced Colitis through Regulation of Inflammatory Response in Intestinal Epithelial Cells. Am J Chin Med. 45(5): 1047–1060. https://doi.org/10.1142/S0192415X17500562

Kimura, T., Y. Horikoshi, C. Kuriyagawa, and Y. Niiyama (2021). Rho/ROCK Pathway and Noncoding RNAs: Implications in Ischemic Stroke and Spinal Cord Injury. Int J Mol Sci. 22(21): 11573. https://doi.org/10.3390/ijms222111573

Koohi, O., R. Shahriarirad, A. Erfani, F. Nekouei, S. Seifbehzad, A. Ebrahimi, N. Tanideh, M. Hosseinzadeh, E. Nadimi, and S. Ashkani-Esfahani (2023). Evaluation of oral and topical bovine colostrum compared to mesalamine in the treatment of animal model of acetic acid-induced ulcerative colitis. Ann Gastroenterol. 36(3): 300–306. https://doi.org/10.20524/aog.2023.079

Kucharzik, T., S. Koletzko, K. Kannengiesser, and A. Dignass (2020). Ulcerative Colitis - Diagnostic and Therapeutic Algorithms. Dtsch Arztebl Int. 117(33-34): 564–574. https://doi.org/10.3238/arztebl.2020.0564

Kuo, W.T., M.A. Odenwald, J.R. Turner, and L. Zuo (2022). Tight junction proteins occludin and ZO-1 as regulators of epithelial proliferation and survival. Ann N Y Acad Sci. 1514(1): 21–33. https://doi.org/10.1111/nyas.14798

Le Berre, C., S. Honap, and L. Peyrin-Biroulet (2023). Ulcerative colitis. Lancet. 402(10401): 571–584. https://doi.org/10.1016/S0140-6736(23)00966-2

Lee, H.W., J.H. Jun, J. Choi, T.Y. Choi, J.A. Lee, L. Ang, H.Y. Go, and M.S. Lee (2020). Herbal prescription for managing menopausal disorders: A practice survey in Korean medicine doctors. Complement Ther Clin Pract. 38: 101073. https://doi.org/10.1016/j.ctcp.2019.101073

Liu, J.Q., W.A. Hao, Y.L. Liu, D. Yang, H.L. Wang, L. Zhao, H. Chen, L. Li, C.L. Jiang, X. Zhou, J. Fu, and Z. Li (2025). The efficacy and active compounds of Chaihuang Qingyi Huoxue granule to Ameliorate intestinal mucosal barrier injury in rats with severe acute pancreatitis by suppressing the HMGB1/TLR4/NF-κB signaling pathway. Int Immunopharmacol. 144: 113632. https://doi.org/10.1016/j.intimp.2024.113632

Liu, X., F. Liang, J. Zhang, Z. Li, J. Yang, and N. Kang (2020). Hyperbaric Oxygen Treatment Improves Intestinal Barrier Function After Spinal Cord Injury in Rats. Front Neurol. 11: 563281. https://doi.org/10.3389/fneur.2020.563281

Liu, Y., B.G. Li, Y.H. Su, R.X. Zhao, P. Song, H. Li, X.H. Cui, H.M. Gao, R.X. Zhai, X.J. Fu, and X. Ren (2022). Potential activity of Traditional Chinese Medicine against Ulcerative colitis: A review. J Ethnopharmacol. 289: 115084. https://doi.org/10.1016/j.jep.2022.115084

Lin, S. N., R. Mao, C. Qian, D. Bettenworth, J. Wang, J. Li, D.H. Bruining, V. Jairath, B.G. Feagan, M. H. Chen, Stenosis Therapy and Antifibrotic Research (STAR) Consortium, and F. Rieder (2022). Development of antifibrotic therapy for stricturing Crohn's disease: lessons from randomized trials in other fibrotic diseases. Physiol Rev. 102(2): 605–652. https://doi.org/10.1152/physrev.00005.2021

Luo, Q., P. Zhou, S. Chang, Z. Huang, and Y. Zhu (2023a). The gut-lung axis: Mendelian randomization identifies a causal association between inflammatory bowel disease and interstitial lung disease. Heart Lung. 61: 120–126. https://doi.org/10.1016/j.hrtlng.2023.05.016

Luo, S., J. He, S. Huang, X. Wang, Y. Su, Y. Li, Y. Chen, G. Yang, B. Huang, S. Guo, L. Zhou, and X. Luo (2022). Emodin targeting the colonic metabolism via PPARγ alleviates UC by inhibiting facultative anaerobe. Phytomedicine. 104: 154106. https://doi.org/10.1016/j.phymed.2022.154106

Luo, Y., Y. Qiu, R. Zhou, Y. Zhang, X. Ji, Z. Liu, R. Li, Y. Zhang, F. Yang, J. Hou, S. Zhang, T. Wang, H. Song, and X. Tao (2023b). Shaoyao Gancao decoction alleviates the central hyperalgesia of recurrent NTG-induced migraine in rats by regulating the NGF/TRPV1/COX-2 signal pathway. J Ethnopharmacol. 317: 116781. https://doi.org/10.1016/j.jep.2023.116781

Marvisi, M., L. Balzarini, C. Mancini, S. Ramponi, C. Marvisi, and E. Maffezzoni (2019). Subclinical Nasal and Lung Lymphocytosis in Ulcerative Colitis. Colitis. Inflamm Intest Dis. 3(4): 187–191. https://doi.org/10.1159/000495985

Paul, N., M. Lazarev, K. Montemayor, and A.J. Horne (2022). Cavitary lung nodules as an extraintestinal manifestation of ulcerative colitis. BMJ Case Rep. 15(9): e251976. https://doi.org/10.1136/bcr-2022-251976

Petagna, L., A. Antonelli, C. Ganini, V. Bellato, M. Campanelli, A. Divizia, C. Efrati, M. Franceschilli, A. M. Guida, S. Ingallinella, F. Montagnese, B. Sensi, L. Siragusa, and G.S. Sica (2020). Pathophysiology of Crohn's disease inflammation and recurrence. Biol Direct. 15(1): 23. https://doi.org/10.1186/s13062-020-00280-5

Sands, B.E., S. Schreiber, I. Blumenstein, M.V. Chiorean, R.C. Ungaro, and D.T. Rubin (2023). Clinician's Guide to Using Ozanimod for the Treatment of Ulcerative Colitis. J Crohns Colitis. 17(12): 2012–2025. https://doi.org/10.1093/ecco-jcc/jjad112

Şen, A., B. Ertaş, Ö. Çevik, A. Yıldırım, D.G. Kayalı, D. Akakın, L. Bitiş, and G. Şener (2023). Cotinus coggygria Scop. Attenuates Acetic Acid-Induced Colitis in Rats by Regulation of Inflammatory Mediators. Appl Biochem Biotechnol. 195(11): 7021–7036. https://doi.org/10.1007/s12010-023-04474-1

Shostak, K., C. Wathieu, S. Tielens, and A. Chariot (2021). NF-κB Signaling in Ex-Vivo Mouse Intestinal Organoids. Methods Mol Biol. 2366: 283–292. https://doi.org/10.1007/978-1-0716-1669-7_17

Wangchuk, P., K. Yeshi, and A. Loukas (2024). Ulcerative colitis: clinical biomarkers, therapeutic targets, and emerging treatments. Trends Pharmacol Sci. 45(10): 892–903. https://doi.org/10.1016/j.tips.2024.08.003

Wang, M., R. Fu, D. Xu, Y. Chen, S. Yue, S. Zhang, and Y. Tang (2024). Traditional Chinese Medicine: A promising strategy to regulate the imbalance of bacterial flora, impaired intestinal barrier and immune function attributed to ulcerative colitis through intestinal microecology. J Ethnopharmacol. 318(Pt A): 116879. https://doi.org/10.1016/j.jep.2023.116879

Wang, S., L. Cai, Y. Ma, and H. Zhang (2025). Shaoyao decoction alleviates DSS - induced colitis by inhibiting IL - 17a - mediated polarization of M1 macrophages. J Ethnopharmacol. 337(Pt 3): 118941. https://doi.org/10.1016/j.jep.2024.118941

Wang, Y., K. You, Y. You, Q. Li, G. Feng, J. Ni, X. Cao, X. Zhang, Y. Wang, W. Bao, X. Wang, T. Chen, H. Li, Y. Huang, J. Lyu, S. Yu, H. Li, S. Xu, K. Zeng, and X. Shen (2022). Paeoniflorin prevents aberrant proliferation and differentiation of intestinal stem cells by controlling C1q release from macrophages in chronic colitis. Pharmacol Res. 182: 106309. https://doi.org/10.1016/j.phrs.2022.106309

Wei, Y.Y., Y.M. Fan, Y. Ga, Y.N. Zhang, J.C. Han, and Z.H. Hao (2021). Shaoyao decoction attenuates DSS - induced ulcerative colitis, macrophage and NLRP3 inflammasome activation through the MKP1/NF - κB pathway. Phytomedicine. 92: 153743. https://doi.org/10.1016/j.phymed.2021.153743

Wu, D., Y. Zhang, B. Zou, Y. Lu, and H. Cao (2023). Shaoyao decoction alleviates TNBS - induced ulcerative colitis by decreasing inflammation and balancing the homeostasis of Th17/Treg cells. BMC Complement Med Ther. 23(1): 424. https://doi.org/10.1186/s12906-023-04237-9

Wu, J., Y. Luo, Y. Shen, Y. Hu, F. Zhu, J. Wu, and Y. Liu (2022a). Integrated Metabonomics and Network Pharmacology to Reveal the Action Mechanism Effect of Shaoyao Decoction on Ulcerative Colitis. Drug Des Devel Ther. 16: 3739–3776. https://doi.org/10.2147/DDDT.S375281

Wu, Y., X. Liu, and G. Li (2022b). Integrated bioinformatics and network pharmacology to identify the therapeutic target and molecular mechanisms of Huangqin decoction on ulcerative Colitis. Sci Rep. 12(1): 159. https://doi.org/10.1038/s41598-021-03980-8

Xie, Q., H. Li, R. Ma, M. Ren, Y. Li, J. Li, H. Chen, Z. Chen, D. Gong, and J. Wang (2022). Effect of Coptis chinensis franch and Magnolia officinalis on intestinal flora and intestinal barrier in a TNBS-induced ulcerative colitis rats model. Phytomedicine. 97: 153927. https://doi.org/10.1016/j.phymed.2022.153927

Xu, J., and N. Lin (2024). HOXD10 regulates intestinal permeability and inhibits inflammation of dextran sulfate sodium-induced ulcerative colitis through the inactivation of the Rho/ROCK/MMPs axis. Open Med (Wars). 19(1): 20230844. https://doi.org/10.1515/med-2023-0844

Yan, J., Y. Tang, X. Zhong, H. Huang, H. Wei, Y. Jin, Y. He, J. Cao, L. Jin, and B. Hu (2021). ROCK inhibitor attenuates carbon blacks-induced pulmonary fibrosis in mice via Rho/ROCK/NF-kappa B pathway. Environ Toxicol. 36(7): 1476–1484. https://doi.org/10.1002/tox.23135

Yin, J., J. Yi, C. Yang, B. Xu, J. Lin, H. Hu, X. Wu, H. Shi, and X. Fei (2021). Chronic atrophic gastritis and intestinal metaplasia induced by high-salt and N-methyl-N'-nitro-N-nitrosoguanidine intake in rats. Exp Ther Med. 21(4): 315. https://doi.org/10.3892/etm.2021.9746

Zeng, Y.Y., and K.Y. Li (2017). Effects of Jiawei Shaoyao - Gancao Decoction and Its Drug - Containing Serum on Proliferation, Apoptosis, and Ultrastructure of Human Adenomyosis Foci Cells. Evid Based Complement Alternat Med. 2017: 7821095. https://doi.org/10.1155/2017/7821095

Zhang, X.Y., H.M. Zhao, Y. Liu, X.Y. Lu, Y.Z. Li, Q.H. Pan, H.Y. Wang, W. Ge, and D.Y. Liu (2021). Sishen Pill Maintained Colonic Mucosal Barrier Integrity to Treat Ulcerative Colitis via Rho/ROCK Signaling Pathway. Evid Based Complement Alternat Med. 2021: 5536679. https://doi.org/10.1155/2021/5536679

Zhang, Y., Y. Ni, and L. Li (2024). The gut-lung axis: Mendelian randomization identifies a causal association between inflammatory bowel disease and interstitial lung disease. Heart Lung 64: 215–216. https://doi.org/10.1016/j.hrtlng.2023.11.015

Zheng, S., T. Xue, B. Wang, H. Guo, and Q. Liu (2022). Chinese Medicine in the Treatment of Ulcerative Colitis: The Mechanisms of Signaling Pathway Regulations. Am J Chin Med. 50(7): 1781–1798.

https://doi.org/10.1142/S0192415X22500756

Zhou, B., W. Li, Y. Li, D. Sun, and X. Du (2024). Effect of Self - developed Ye'an Analgetic Decoction/Jiawei Shaoyao Gancao Decoction Combined with Tramadol on TCM Symptom Scores and RLS Severity of patients with Restless Legs Syndrome. Pak J Med Sci. 40(5): 1017–1021. https://doi.org/10.12669/pjms.40.5.8400

Zhou, L., L. Zhu, X. Wu, S. Hu, S. Zhang, M. Ning, J. Yu, and M. Chen (2023). Decreased TMIGD1 aggravates colitis and intestinal barrier dysfunction via the BANF1-NF-κB pathway in Crohn's disease. BMC Med. 21(1): 287. https://doi.org/10.1186/s12916-023-02989-2

Zhou, R., Y. Huang, C. Tian, Y. Yang, Z. Zhang, and K. He (2023). Coptis chinensis and Berberine Ameliorate Chronic Ulcerative Colitis: An Integrated Microbiome-Metabolomics Study. Am J Chin Med. 51(8): 2195–2220. https://doi.org/10.1142/S0192415X23500945

Zhuang, H., Q. Lv, C. Zhong, Y. Cui, L. He, C. Zhang, and J. Yu (2021). Tiliroside Ameliorates Ulcerative Colitis by Restoring the M1/M2 Macrophage Balance via the HIF - 1α/glycolysis Pathway. Front Immunol. 12: 649463. https://doi.org/10.3389/fimmu.2021.649463